



# Inferring the source of evaporated waters using stable H and O isotopes

Gabriel J. Bowen<sup>1</sup> · Annie Putman<sup>1</sup> · J. Renée Brooks<sup>2</sup> · David R. Bowling<sup>3</sup> · Erik J. Oerter<sup>4</sup> · Stephen P. Good<sup>5</sup>

Received: 7 August 2017 / Accepted: 5 June 2018 / Published online: 28 June 2018  
© Springer-Verlag GmbH Germany, part of Springer Nature 2018

## Abstract

Stable isotope ratios of H and O are widely used to identify the source of water, e.g., in aquifers, river runoff, soils, plant xylem, and plant-based beverages. In situations where the sampled water is partially evaporated, its isotope values will have evolved along an evaporation line (EL) in  $\delta^2\text{H}/\delta^{18}\text{O}$  space, and back-correction along the EL to its intersection with a meteoric water line (MWL) has been used to estimate the source water's isotope ratios. Here, we review the theory underlying isotopic estimation of source water for evaporated samples ( $i\text{SW}_E$ ). We note potential for bias from a commonly used regression-based approach for EL slope estimation and suggest that a model-based approach may be preferable if assumptions of the regression approach are not valid. We then introduce a mathematical framework that eliminates the need to explicitly estimate the EL–MWL intersection, simplifying  $i\text{SW}_E$  analysis and facilitating more rigorous uncertainty estimation. We apply this approach to data from the US EPA's 2007 National Lakes Assessment. We find that data for most lakes are consistent with a water source similar to annual runoff, estimated from monthly precipitation and evaporation within the lake basin. Strong evidence for both summer- and winter-biased sources exists, however, with winter bias pervasive in most snow-prone regions. The new analytical framework should improve the rigor of  $i\text{SW}_E$  in ecohydrology and related sciences, and our initial results from US lakes suggest that previous interpretations of lakes as unbiased isotope integrators may only be valid in certain climate regimes.

**Keywords** Stable isotopes · Ecohydrology · Water source · Evaporation · Bayesian methods

---

Communicated by Todd E Dawson.

✉ Gabriel J. Bowen  
gabe.bowen@utah.edu

<sup>1</sup> Department of Geology and Geophysics and Global Change and Sustainability Center, University of Utah, Salt Lake City, UT 84112, USA

<sup>2</sup> Western Ecology Division, National Health and Environmental Effects Research Laboratory, Office of Research and Development, U.S. Environmental Protection Agency, Corvallis, OR, USA

<sup>3</sup> Department of Biology and Global Change and Sustainability Center, University of Utah, Salt Lake City, UT 84112, USA

<sup>4</sup> Lawrence Livermore National Laboratory, Livermore, CA 94550, USA

<sup>5</sup> Department of Biological and Ecological Engineering, Oregon State University, Corvallis, OR, USA

## Introduction

A common and cross-cutting application of stable isotopes in many fields is the determination of elemental sources or partitioning of sources within a mixture. Stable H and O isotopes of waters have long been used in hydrology to partition recharge and discharge sources (Clark and Fritz 1997; Kendall and McDonnell 1998). Beginning in the 1990s, James Ehleringer and his students and colleagues extended this concept to the determination of water sources used by plants (Dawson and Ehleringer 1991; Ehleringer et al. 1991; Ehleringer and Dawson 1992; Dawson and Pate 1996; Dawson 1998; Williams et al. 2005; Roden and Ehleringer 2007). Applications in each of these areas have grown in number and scope over the past three decades, and a series of recent field studies and meta-analyses have advanced fundamental new concepts that may govern global-scale partitioning within hydroclimatic and ecohydrological systems (Henderson and Shuman 2009; Evaristo et al. 2015; Good et al. 2015a). At the same time, new applications, for example, in

the realm of urban and human-managed systems, have continued to emerge (Good et al. 2014; Ehleringer et al. 2016; Jameel et al. 2016; Tipple et al. 2017).

Natural spatial and temporal variation in the stable isotope ratios of H and O ( $\delta^2\text{H}$  and  $\delta^{18}\text{O}$ , respectively; defined below) is a common feature of most hydrological systems. This variation arises primarily due to changing atmospheric conditions, which affect the transport of heavy and light isotopes in atmospheric moisture to a given region of the continents at a given time (Dansgaard 1964; Gat 1996). Values of most fresh waters array along a meteoric water line (MWL) with a slope of  $\sim 8$  in H and O isotope space that can be characterized through the measurement of global (GMWL) or local (LMWL) precipitation samples (Fig. 1a; Craig 1961). These MWLs establish the reference frame for identification of sources water (SW) contributing to a sample, and have been applied to interpret data from samples as diverse as aquifer, lake and stream waters, plant xylem waters, milk and fruit juices, and human body water (Henderson and Shuman 2009; Chesson et al. 2010; Evaristo et al. 2015; Oerter et al. 2017).

Stable H and O isotopes are well suited to these applications because they are largely conservative tracers, maintaining their isotopic ratios despite other physical and chemical transformations undergone by the water they are carried in. The primary exception to this conservative behavior results from the effects of evaporation. Strong discrimination against the heavy isotopes of H and O during the formation of vapor from liquid water can produce large shifts in the isotopic values of the remaining liquid (Fig. 1a, Craig and

Gordon 1965). Fortunately, kinetic effects during evaporation produce a systematic deviation of residual (“evapoconcentrated”) water values from the MWL, which can be used to detect the influence of evaporation (Fig. 1a; Craig and Gordon 1965; Gat 1996). As evapoconcentration of a pool of water proceeds its isotopic composition will evolve along an “evaporation line” (EL) that trends away from the MWL with a slope lower than 8, giving diagnostic values of “deuterium excess” ( $D\text{-excess} = \delta^2\text{H} - 8 \times \delta^{18}\text{O}$ ) lower than rainwater values (approximately  $+10\text{‰}$ ). If the slope of the EL affecting a given sample or collection of samples is known, this provides a basis for ‘correcting’ the evaporation effects by back-projecting the H and O isotope values along the evaporation line to its intersection with the MWL, giving the isotopic composition of the sample source water prior to evapoconcentration (Fig. 1a).

As the application of water isotopes to source water determination problems, particularly those involving evapoconcentration, has grown, methodological and data interpretation challenges have emerged. First, evaporation line slopes can vary widely due to the different expressions of kinetic effects among systems, and range from values of  $\sim 2.5$  in soils to values greater than 6 over large water bodies exposed to strong winds (Gat 1996; Gibson et al. 2008). Different approaches have been used in the literature to estimate the slope value appropriate to a given dataset, ranging from calculations based on theoretical models to experimental pan-evaporation trials to fitting “evaporation lines” using multiple data from the study system. Second, quantitative assessment of uncertainty has grown in importance as many

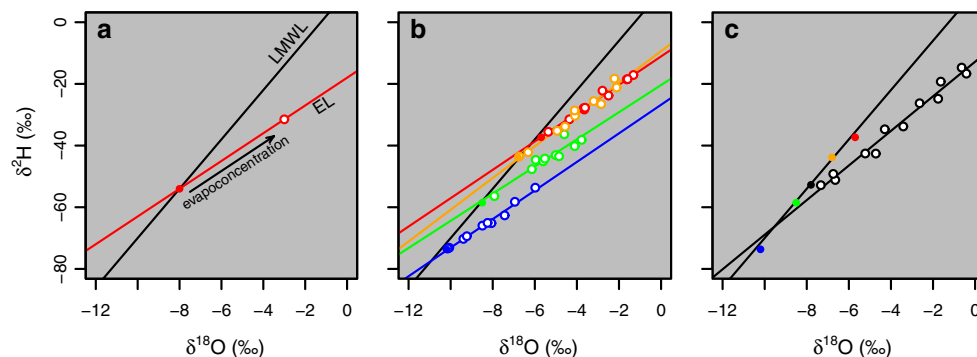


**Fig. 1** Hypothetical examples illustrating  $i\text{SW}_E$  applications. **a** Theoretical framework. Source water values (solid red circle) lie along a local meteoric water line (LMWL). An evapoconcentrated water sample (open red circle) has H and O isotope ratios that have evolved relative to the source along an evaporation line (EL). Measured source values are back-projected along the EL to its intersection with the LMWL to estimate the source water values. **b** Multiple water samples (open symbols) derived from one of four different ‘source waters’ (solid circles) with random noise and without mixing. In this case, a regression line fit to each group of evapoconcentrated water samples approximates the evaporation line slope (true value of  $4.5 \pm 0.5$ , estimated values between 4.24 and 4.74) and projects to an intersection

with the LMWL approximating the actual source water value. **c** Multiple evapoconcentrated water samples (open symbols) derived from varying mixtures of the four sources shown in **b**. The model shown includes sinusoidal variation in source water values that is positively correlated with evapoconcentration, reflecting correlated seasonal variation in source water isotope ratios and evaporative losses. In this case, the regression fit over-estimates the EL slope (5.5) and the intercept between this line and the LMWL gives an estimate of the source water isotope values that is lower than the true average value (black solid circle). This figure is available in color in the online version of the journal

of these applications have moved from early ‘case studies’ to larger scale, meta-analytical syntheses. Again, a range of approaches has been adopted, but few studies have undertaken rigorous and comprehensive error assessment. The complexity of the source inference problem when evaporation is considered leads to challenges in the analytical propagation of error.

Here, we provide a critique of isotopic methods used for isotopic inference of source water for evapoconcentrated samples (iSW<sub>E</sub>) and propose a new conceptual framework with recommendations that address challenges emerging from recent work. We describe implementations of this framework in software for the R programming environment that support data analysis for three common application classes. Lastly, we apply the framework to a large water isotope dataset for lakes and reservoirs across the contiguous USA to revisit previous regional work (Henderson and Shuman 2009) that had suggested limited seasonal bias of lake water recharge, and describe the implications of our new results for ecohydrological and paleoclimatic research.

## Foundation

Isotope ratios of H and O, reported on the Vienna Standard Mean Ocean Water/Vienna Standard Light Antarctic Precipitation reference scale in  $\delta$  notation [ $\delta = (R_{\text{sample}}/R_{\text{standard}} - 1)$ , where  $R = {}^2\text{H}/{}^1\text{H}$  or  ${}^{18}\text{O}/{}^{16}\text{O}$ ], vary systematically across landscapes due to the influence of factors such as temperature gradients, topography, and convective and frontal lifting on rainout (Rozanski et al. 1993). The patterns resulting from these processes were described more than a half-century ago as ‘continental’, ‘latitude’, and ‘altitude’ effects (Dansgaard 1964), each describing the tendency of air masses that are progressively removed from low-latitude, marine vapor sources to have decreasing relative concentrations of the heavy isotopes  ${}^2\text{H}$  and  ${}^{18}\text{O}$ . These patterns are expressed over both space and time, meaning that both mean annual and seasonal patterns of precipitation water isotope ratios express systematic variation reflecting changes in ‘distance’ to source. The implication for determining SW is the existence of strong and, to a large degree, predictable spatiotemporal patterns in precipitation isotope ratios that are useful for partitioning the sources of water to aquifers, streams, cities, plants, and animals (Bowen and Wilkinson 2002; Bowen 2008; Bowen and Good 2015).

As with any source identification or partitioning problem, isotopic SW determination depends on the assumption of conservative tracer behavior. Although exceptions exist (Lin et al. 1993; Ellsworth and Williams 2007; Zhao et al. 2016) and recent work has hinted at new complexity yet to be understood (Oerter et al. 2014), stable water isotopes are often nearly ideal in this respect. The primary exception

to this conservative behavior is the fractionating influence of evaporation. As described in the introduction, evapoconcentration preferentially removes the lighter isotopes of H and O, producing a positive shift in the isotope ratios of the residual liquid along an EL. Because the size of this effect is proportionally larger for O than H, ELs deviate from the MWL. If the slope of the EL can be estimated, we can correct for evapoconcentration effects and reconstruct ‘un-evaporated’ source water isotope ratios (Fig. 1a).

## Estimating EL slope

Two approaches are now commonly, if not exclusively, used to estimate EL slopes for iSW<sub>E</sub> applications. Each is founded on a set of assumptions, and these are often not clearly acknowledged or critically evaluated in published work. At best, the result is a lack of clarity and transparency of the limitations of a particular application; at worst, erroneous results can be obtained if the study conditions are inconsistent with the assumptions that are made.

Perhaps the most common approach to EL estimation is the use of multiple samples, distributed over space or time, to characterize evapoconcentration of water isotopes in a system (Fig. 1b). The fundamental assumption underlying this approach is that isotopic variation in the sample set results solely from variation in the degree of evapoconcentration, and that all samples have a common source. This condition is perhaps best reflected in pan-evaporation studies (e.g., Welhan and Fritz 1977), where a volume of water is introduced to an open container and allowed to progressively evapoconcentrate. Repeat sampling of this volume documents evapoconcentration effects on the isotopic values of residual water, and allows for estimating the EL. Unfortunately, in many natural systems, the pan-evaporation experiment is a poor analog. In particular, the assumption that water in soils, rivers, and smaller lakes has a fixed initial composition, and exhibits isotopic variation in response to temporal changes in the degree of evapoconcentration alone, is seldom true. Violation of this assumption, as in the case where source water compositions and the degree of evapoconcentration are correlated (e.g., over seasonal cycles), can give rise to significant and systematic biases in EL slope and source water isotope ratio estimates (Fig. 1c). Although the nature of these biases could vary among systems, perhaps the most common mode would be where isotopically lighter sources (e.g., cooler season or higher elevation) exhibit less evapoconcentration, leading to a light-bias in iSW<sub>E</sub> estimates (Fig. 1c).

The regression approach is appealing because of its simplicity, and has been used extensively. For example, Henderson and Shuman (2009) used sampling of lakes in the western USA to document isotopic variation in these systems. The results for lakes within close geographic proximity

were arrayed along lines with  $\delta^2\text{H}/\delta^{18}\text{O}$  slopes lower than those of regional meteoric water lines, and were interpreted to reflect seasonal variation in the evapoconcentration of lake water and used to estimate the ELs associated with this process. Similar logic was applied to USA river water data by Kendall and Coplen (2001). Comparison of results suggested that river source water tended to be more  $^2\text{H}$ - and  $^{18}\text{O}$ -depleted than those of lakes, implying that hydrological processes biased river discharge toward winter season snowmelt, whereas lakes in the same regions were filled by more seasonally representative runoff (Henderson and Shuman 2010).

More recently, a meta-analysis by Evaristo et al. (2015) used regression of xylem water measurements from multiple samples (obtained from multiple individual plants over time or space, depending on study) to estimate EL slopes. Xylem water is particularly challenging for the EL regression approach because plants have the potential to use a mixture of water from multiple pools with different unevaporated source water isotope ratios, and each plant may have a unique mixture of these sources. This difference in mixing ratios over time or space violates the EL regression assumption of a common source for all samples. Users of this approach need to critically evaluate this assumption for each application and should work to demonstrate that observed isotopic variation in their study system represents variation in evapoconcentration alone. One component of such a demonstration could be to compare EL regression results with theoretical modeling of EL slopes, described below.

A second approach to EL slope estimation involves theoretical modeling of evaporative isotopic fractionation based on the model of Craig and Gordon (1965). This model describes the balance of equilibrium and kinetic isotope effects that determine the EL slope in terms of isotope ratios of the liquid and ambient atmospheric vapor and physical properties of the air–water interface (Gat and Bowser 1991; Gat 1996; Gibson et al. 2008). The primary challenges involved in applying the theoretical method lie in the specification of model parameters. One particularly difficult-to-estimate parameter is the atmospheric water vapor isotope ratio, which affects the isotopic composition of the net evaporative flux through its contribution to bi-directional diffusive vapor exchange within the boundary layer. For large-scale, multi-site studies atmospheric values are not usually available from measurements and are often estimated assuming equilibrium with precipitation (e.g., Gibson et al. 2008; see, however, Good et al. 2015b). A second challenge is the specification of model parameters that are representative of atmospheric conditions governing the balance of kinetic vs. equilibrium fractionation, given that real-world conditions vary significantly over time and between systems (e.g., soil vs. open water). Here, the sampling-based

approach has a significant advantage, in that under ideal circumstances the natural samples gathered to describe the EL integrate temporal variation in evaporation conditions. For the model-based approach, the primary assumption is that a set of representative model conditions can be prescribed which reflect the flux-weighted influence of evaporation on the residual water mass.

The model-based approach is less frequently applied in field studies, but is a common choice in large-scale syntheses and modeling studies. Good et al. (2015a), for example, recently modeled evaporative fractionation of H isotopes in a global-scale isotopic water balance. In this study, the balance between soil and surface water evaporation was a variable specifically targeted in the modeling, and the strong contrast in fractionation between evaporation occurring in these two environments was used as a diagnostic signature. The results, together with other recent studies (e.g., Brooks et al. 2010; Goldsmith et al. 2012; Evaristo et al. 2015; Oerter and Bowen 2017), suggest that the expression of soil water evaporation effects in groundwater and stream water isotope ratios may be modulated by limited and variable connectivity between soil ‘immobile’ and ‘mobile’ water pools. This potentially complicates the specification of parameters for the model-based approach given that the contribution of soil and open-water evaporation to the evapoconcentration of stream, ground, and lake water systems is both variable and uncertain. Nevertheless, the theoretical approach for estimating the EL slope is really the only feasible method for large-scale synthesis and modeling studies. We also believe that this approach should be more frequently adopted in site-based studies as an alternative to regression, particularly in situations where the assumptions of that method are questionable or to validate regression-based ELs. To facilitate this, we have made the gridded theoretical estimates of evaporation-weighted EL slopes for the USA used in our case study below web-accessible.

### Testing water origin

Once an EL equation has been determined, most studies determine SW as the intersection between that line and the LMWL or GMWL (Fig. 1a). The inferred SW values can be evaluated directly as representative of a proximal water source (e.g., lake inflow water), but in most cases will reflect a mixture of sources of interest to researchers (e.g., summer and winter runoff). In the latter case, inferred SW isotope ratios will reflect a (linearly) weighted mixture of the water sources, and can be used to estimate mixing ratios for the different sources. In most cases, such mixing analyses will be underdetermined, in that multiple source/mixture combinations could give similar inferred SW isotope values, and results of the analysis will be sensitive to how the individual sources are defined.

The most common approach to interpreting estimated SW values is to compare them with values for one or more hypothesized sources to test whether the observed values are consistent with a proposed source or compare between multiple potential sources. The papers by Evaristo et al. (2015) and Henderson and Shuman (2009, 2010) both adopt the former approach: comparing EL reconstructed source water values for plants, lakes, or rivers with local or basin-averaged annual precipitation isotope ratios to assess whether the observed waters reflected an unbiased average of precipitation. Good et al. (2014) offer an example of the second approach, comparing tap water sampled in communities across the western USA with precipitation and river water isotope ratios to evaluate the relative likelihood that cities and towns used water from their local basin vs. water imported from outside of their basin.

Robust tests involving  $iSW_E$  estimates require knowing the uncertainty of these estimates. Characterization of uncertainty is challenging to achieve, and different studies have applied different levels of rigor. One approach has been to use the ordinary least squares estimates of the uncertainty in regression-derived EL slopes and intercepts to estimate the uncertainty in the EL/MWL intersection (e.g., Henderson and Shuman 2009). Although simple and tractable, this approach offers an incomplete assessment in that it ignores uncertainty in the water sample data themselves, the MWL, and any hypothesized water sources, as well as interactions between the uncertainties in these quantities. Moreover, this approach is typically applied to estimate uncertainty in SW isotope ratios for each element independently, and does not offer a straightforward way of assessing covariance in source water H and O isotope estimates or their impact on subsequent inference from these values. Good et al. (2014) provide a rare example of a comprehensive assessment in their tap water study, which uses a full Bayesian inversion incorporating uncertainty in each of these parameters. Although potentially generalizable, their analysis framework is relatively complex and, as we suggest below, could be streamlined without loss of information or power for many applications.

## Analytical framework

### Theory

To facilitate future applications, a simple, generalizable framework for conducting common types of water source tests with comprehensive assessment of uncertainty is needed. In the following sections, we propose such a framework and describe its implementation for common types of source water tests. Our proposed framework begins with the recognition that most  $iSW_E$  applications can be simplified to a comparison of a ‘true’

EL slope estimated for a study system (as described above) with the EL slope implied by isotope values for an evapoconcentrated sample and a hypothesized source water.

Consider a hypothetical example where the goal is to test whether recent, local precipitation is likely to be the source of water to a tree with observed xylem water values  $\delta^2H_o$  and  $\delta^{18}O_o$ . In the traditional framework, the intersection of the EL (defined by the observed values and an EL slope estimated using one of the methods described above) with a MWL would first be calculated, and these values would be taken to represent the true un-evaporated source water ( $\delta^2H_s$  and  $\delta^{18}O_s$ ). Then, the estimated source values would be compared with the isotopic values for the hypothesized precipitation source ( $\delta^2H_h$ ,  $\delta^{18}O_h$ ) to obtain a statistical estimate of similarity or dissimilarity. This approach involves two steps, each of which involves the estimation and propagation of correlated uncertainties in bi-variate isotope space.

This analysis framework can be simplified considerably if one condenses the inferential sequence above, recognizing that at the root of the analysis is the comparison of two sets of points in H/O isotope space, each of which defines a line. Under conditions where the water isotopes behave conservatively with the exception of evapoconcentration effects (the fundamental assumption for  $iSW_E$ ), the observed sample values and true source water values are connected by the true evaporation line, with slope  $m_t$ . For any hypothesized source water, a second, hypothesized, EL can be defined that connects this water’s H/O isotope values with  $\delta^2H_o/\delta^{18}O_o$ . If the hypothesized source is the true source, then it is necessary and sufficient that: (1) the slope of the hypothesized EL ( $m_h$ ) is equal to  $m_t$ , and (2) both isotope ratios of the observed sample are greater than those of the hypothesized source (i.e., under normal conditions, evapoconcentration can only produce a positive shift in H and O isotope values).

Evaluation of hypothesized source water compositions can be conducted using Bayes’ Theorem:

$$P(A|B) = \frac{P(B|A)P(A)}{P(B)}$$

In this case, we are interested in the probability that  $\{\delta^2H_h, \delta^{18}O_h\}$  represents the true source water values (A) given the observed sample values  $\{\delta^2H_o, \delta^{18}O_o\}$  (B). The relative value of conditional probability  $P(B|A)$  can be evaluated with reference to the conditions given above, specifically:

$$P(B|A) = P(m_h = m_t) \propto \frac{1}{\sqrt{2\pi\sigma_t^2}} e^{-\frac{(m_h - \bar{m}_t)^2}{2\sigma_t^2}}, \tag{1a}$$

where  $\bar{m}_t$  and  $\sigma_t$  are the mean and standard deviation of the distribution for the true EL slope, and

$$P(B|A) = 0 \text{ IF } \delta^2H_o < \delta^2H_h \text{ OR } \delta^{18}O_o < \delta^{18}O_h. \tag{1b}$$

In the applications below, we conduct Monte Carlo sampling from the prior distribution for the source water values [ $P(A)$ ] and the observed water sample value distribution, and evaluate Eqs. 1a, 1b for the value of  $m_h$  corresponding to each Monte Carlo sample. These values are divided by the maximum value of the PDF for  $m_t$  (substituting  $m_h = \bar{m}_t$  in Eq. 1a) to give relative values of conditional probability for each draw. The standardized values are either aggregated for illustration purposes or used to weight individual sample contributions to the posterior probability distribution  $P(A|B)$ , depending on the application.

One key feature of this formulation of the iSW<sub>E</sub> problem is that it eliminates the need to estimate the true source water isotope ratios, reducing the two-part process of the traditional framework to a single step. Although  $\delta^2\text{H}_s$  and  $\delta^{18}\text{O}_s$  can be estimated as an outcome of the analysis, the new framework allows (and requires) the user to more explicitly consider the goals of their analysis and how any external constraints on possible source water values [i.e.,  $P(A)$ ] are specified.

### Implementation for common iSW<sub>E</sub> problems

We describe and provide code for three implementations of the above framework that address common iSW<sub>E</sub> problems. The first deals with assessing the probability that a single potential hypothesized source represents the true source of an observed water (“single source”). The second allows estimation of the most likely source water values along a MWL (“MWL source”). The third deals with mixtures of two or more hypothesized sources. All are coded in the R programming language (R Core Team 2017), and source code is available at <https://github.com/SPATIAL-Lab/watercompare>.

We use bi-variate normal probability distributions to represent the observed sample and hypothesized source water isotope ratios (except for source water in the MWL source case, see below) and a univariate normal distribution to represent  $m_t$ . The use of multivariate distributions is important in that strong covariance between  $\delta^2\text{H}$  and  $\delta^{18}\text{O}$  values in natural systems has significant implications for uncertainty in iSW<sub>E</sub> applications. In cases where uncertainty in the sample or source values arises only from analytical instrument error the variance in isotope parameter estimates may be uncorrelated, but for most other cases (e.g., where sample or source values are estimated from a model or where there is uncertainty arising from spatial or temporal integration of estimated values), the H/O isotope covariance will be strong. The use of normal distributions, as adopted here, may not be appropriate for all potential applications but can easily be changed without compromising the analysis framework.

For the single-source implementation, random Monte Carlo is used to draw a large number of samples from the source and sample distributions. For each draw,  $P(B|A)$  is evaluated as described above, and the mean of these conditional probabilities across all draws is used to represent the Bayesian update to the prior probability for the source. Here and elsewhere, we treat the marginal probability of the observed value ( $P(B)$ ) as unity, and the resulting posterior is best considered to represent the relative weight of support for a given hypothesized source. The hypothetical case illustrated in Fig. 2 shows prior probabilities (Fig. 2a) and relative conditional probabilities (Fig. 2b) associated with 250 draws for a case in which the mean of the hypothesized source water distribution lies near, but not at, the intersection of the EL and MWL. The mean relative conditional probability for this case, 0.61, suggests that the hypothesized source is 61% as likely to be the true source as an idealized, perfectly known source for which average values of  $m_h$  and  $m_t$  are identical, providing relatively strong support for the viability of the hypothesis. The conditional for this case could similarly be compared with an equivalent value for a second hypothesized source to generate an odds ratio and evaluate the relative support for the two sources.

We conducted a sensitivity test of this implementation to assess the discriminatory power given parameter uncertainties reflecting potential real-world applications. For each parameter set, we analyzed a series of hypothesized sources lying along the GMWL and compared the distribution of mean conditional probabilities for different parameter sets. The results show the greatest sensitivity to variation in the uncertainty of the slope and hypothesized source parameters (Fig. 3). Unsurprisingly, isotopic evidence will have the strongest discriminatory power for iSW<sub>E</sub> where these parameters are well constrained, e.g., through pan-evaporation studies and direct measurement of hypothesized sources. Scenarios representing model-derived parameter estimation, for example, show much broader distribution of mean conditional probabilities across potential source values. Slope uncertainty is interactive with the isotopic separation between hypothesized source and sample values (i.e., the extent of evaporative enrichment), such that for highly evapoconcentrated samples with poorly characterized ELs, the conditional probability offers relatively little information (not shown). Lastly, because of the acute angle of intersection between ELs and MWLs the distribution of conditional probabilities across the range of hypothesized source water values is left-skewed (Fig. 3), and this skew is stronger for higher values of  $m_t$  (e.g., stronger for open-water evaporation than for soil evaporation; not shown). Thus, the discriminatory power of the method is greater for hypothesized sources that have isotopic values higher than the ‘true’ source than for those with lower values. This asymmetry reflects the true

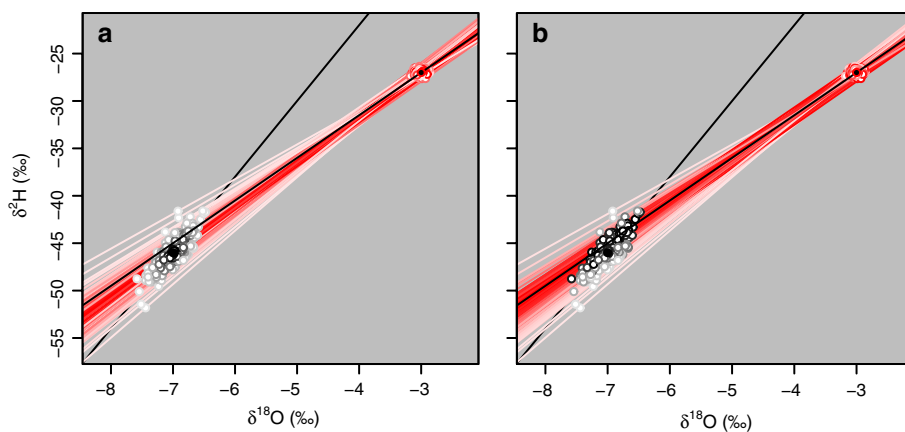


**Fig. 2** Hypothetical application of single-source  $iSW_E$  implementation. **a** First 250 simulated draws from sample and source water distributions with values  $\{\delta^2H_{mean}, \delta^{18}O_{mean}, \delta^2H_{sd}, \delta^{18}O_{sd}, Cov\}$  of  $\{-27, -3, 0.25, 0.05, 0\}$  and  $\{-46, -7, 1.6, 0.2, 0.8\}$ , respectively. Conditional probabilities were evaluated against an EL with slope  $4.5 \pm 0.3$ . The black line in background is the GMWL, red-outlined circles are mean (black fill) or simulated (white) sample values, black-outlined

circles are mean (black fill) or simulated (white) source water values, and red lines are hypothesized ELs for each Monte Carlo draw. Darkness of the lines and symbol outlines scale linearly with the source water prior probability of each draw  $[P(A)]$ . **b** As in **a**, except that darkness of lines and symbol outlines scale linearly with the relative conditional probability of each draw  $[P(B|A)]$ . This figure is available in color in the online version of the journal

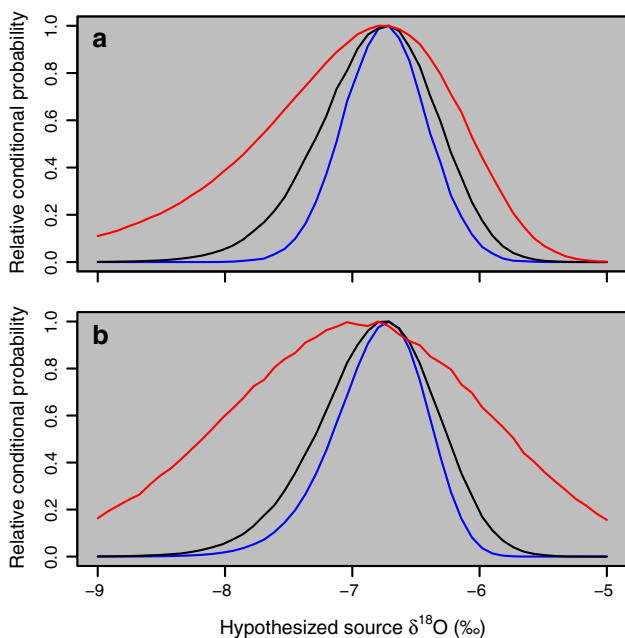


**Fig. 3** Sensitivity test of single-source  $iSW_E$  implementation. **a** Sensitivity test showing posterior probabilities for hypothesized source waters with mean values on the GMWL. Parameters are as in Fig. 2 (black line), or as in Fig. 2 except for the standard deviation of the EL slope (0.1 for the blue curve and 1.0 for the red curve). **b** As in **a**, except the EL slope uncertainty is 0.3 for all curves and hypothesized source water uncertainties  $(\delta^2H_{sd}, \delta^{18}O_{sd}, Cov)$  are  $\{0.25, 0.05, 0\}$  and  $\{5, 0.5, 0.8\}$  for the blue and red curves, respectively. This figure is available in color in the online version of the journal

information content of the  $iSW_E$  method, and should be considered critically in the interpretation of results.

The MWL source implementation simulates the prior distribution of potential source water values by drawing from a distribution around a default or user-supplied MWL equation (Fig. 4). The default equation is a re-calculation of the GMWL ( $\delta^2H = 8.01 \times \delta^{18}O + 9.57$ ) made here based on data from 80,672 globally distributed precipitation samples compiled in the Waterisotopes.org database ([http://wateriso.utah.edu/waterisotopes/pages/spatial\\_db/SPATIAL\\_DB.html](http://wateriso.utah.edu/waterisotopes/pages/spatial_db/SPATIAL_DB.html)). These data were screened to retain only samples with  $d$  between  $-10$  and  $+30\%$ . A user-supplied local meteoric water line can easily be substituted as an argument to the MWL source water function, and will offer a more appropriate representation of potential source water values for regions where precipitation values deviate from the GMWL. The algorithm draws iteratively from the prior distribution of source water values. For each draw, a relative conditional probability is calculated by drawing from the observed sample distribution, calculating  $m_t$ , and obtaining the probability density for that value given the distribution prescribed for  $m_t$ . Draws are retained randomly in proportion to their conditional probability and the process repeated to build a large sample of values representing the posterior distribution. The resulting posterior distribution can be analyzed to generate one or more estimates of the most likely source water values (e.g., for the example case the median value =  $-47.5$  and  $-7.5\%$  for  $\delta^2H$  and  $\delta^{18}O$ , respectively) as well as credible intervals for these estimates (Fig. 4).

A final implementation of the new framework allows estimation of the mixture of two or more waters that best represents the source of an evaporated water sample (e.g., Corbin

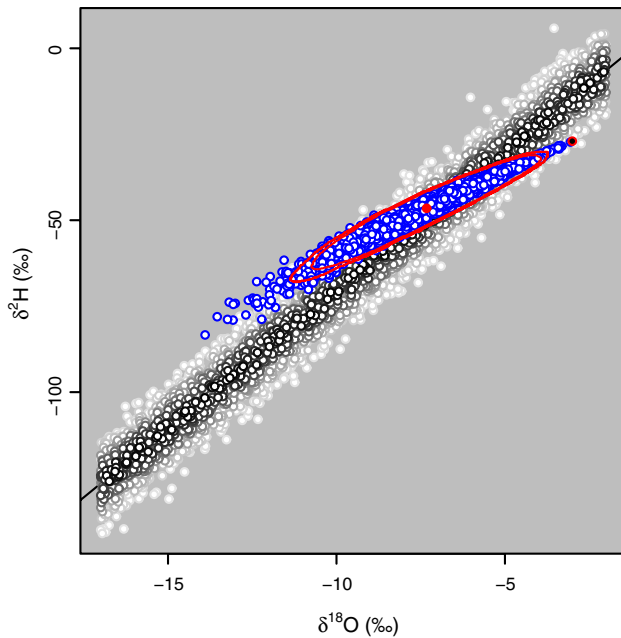


**Fig. 4** Hypothetical application of MWL source  $iSW_E$  implementation. White-filled circles with black/gray outlines show the prior distribution of potential source values. These are generated by drawing  $\delta^{18}O_h$  from a uniform distribution and drawing accompanying  $\delta^2H_h$  values from a normal distribution specified by the mean and standard error of the GMWL equation at the given value of  $\delta^{18}O_h$ . Darkness of the symbol outlines scales linearly with the prior probability of that source value. Circles with blue outlines show posterior distribution of 10,000 potential source values. Red-outlined black circle shows the observed sample value, and the red filled circle and lines show the median and 90 and 95% credible regions for the posterior distribution. Observed sample values and slope used the simulation are as in Fig. 2. This figure is available in color in the online version of the journal

et al. 2005; Bijoor et al. 2012). In this case, the required information includes the isotopic compositions of two or more source waters plus a prior on the mixing ratio of the sources. The implementation uses a Dirichlet distribution to represent the prior on the mixing ratio, specified as a vector of dimensionless values giving the estimated proportional contributions of each source ( $p$ ) and a shape parameter ( $s$ ). Default values of  $s=2$  and  $p=\{1, \dots\}_{1:n}$  are used if no user-specified parameters are given. The Dirichlet parameter for source  $i$  is then calculated as  $\alpha_i = p_i / \min(p) \times s$ . As in the MWL source implementation, the conditional probability associated with each draw is evaluated and the draw is retained randomly in proportion to that probability. To avoid extremely long analysis times and/or return of spurious results for poorly posed analyses the algorithm terminates if more than 1000 draws have been conducted and the fraction of draws retained falls below 1%.

The posterior distribution is output as a distribution of source mixtures (Fig. 5) and can be compared with the prior distribution to test for significant updates to the prior

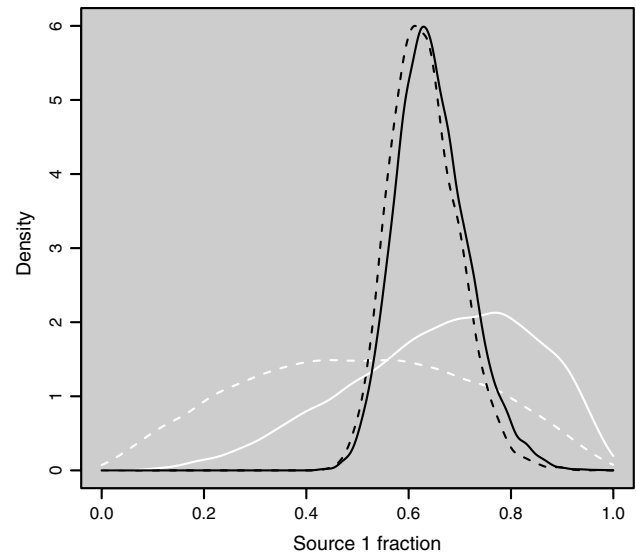


**Fig. 5** Hypothetical application of the mixtures implementation of the  $iSW_E$  method. The analysis estimates the relative contribution of two source waters—source 1  $\{-80, -9, 1.6, 0.2, 0.8\}$  and source 2  $\{-14, -3, 1.6, 0.2, 0.8\}$ —to an observed, evapoconcentrated sample with isotopic value and EL slope as in Fig. 2. White lines show the density of the prior estimates of the mixtures, and the black lines give the kernel density of the posterior based on 10,000 samples. For dashed lines the prior mixture was a Dirichlet distribution with parameter values  $\{2, 2\}$  and for solid lines the parameters were  $\{4, 2\}$

estimate or differences relative to some reference mixture. For well-constrained problems, the implementation shows limited sensitivity to the specified prior (compare solid and dashed posteriors in Fig. 5), although use of a more accurate prior substantially reduces the number of draws required to populate the posterior (e.g., by  $\sim 25\%$  for the solid vs. dashed prior shown in Fig. 5).

## Lake water recharge

### Approach

We illustrate the new  $iSW_E$  approach through analysis of a published dataset representing 1157 lakes distributed across the contiguous USA (Fig. 6; Brooks et al. 2014). Previous work demonstrated that significant evaporative fractionation was reflected in many of the isotopic samples and used these data to estimate evaporation: inflow ratios across the sample set. Here, we analyze the data relative to isotopic estimates for up-catchment precipitation inputs to ask whether lakes across the network reflect the isotopic composition of precipitation within their drainage basins and whether they suggest any bias toward summer or winter season precipitation (Fig. 6). The R code used to conduct each step of the



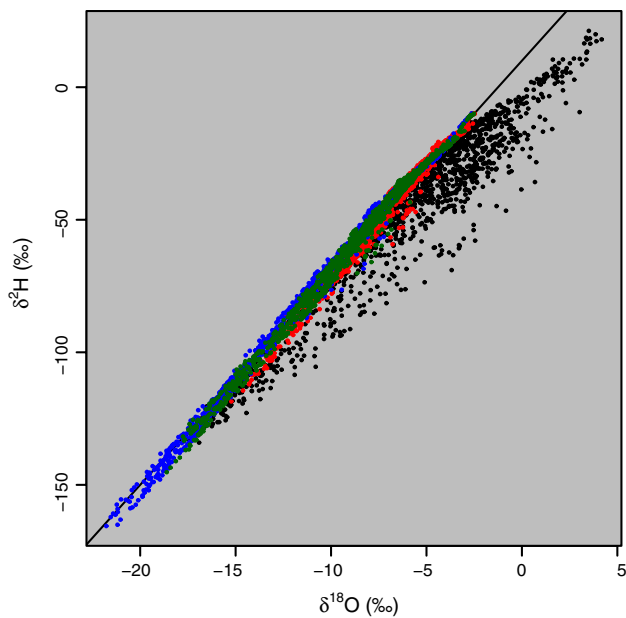


**Fig. 6** Data and source water estimates for the EPA 2007 lake analysis. Black dots: average water isotope data for 1141 lakes within the contiguous USA. Other symbols show the estimated runoff-weighted, catchment-average precipitation isotope ratios for each site for summer (red), winter (blue), and the full 2007 water year (green). This figure is available in color in the online version of the journal

analysis is available at <https://github.com/SPATIAL-Lab/watercompare>.

Multiple measurements for a subset of 95 lakes that were sampled twice during the 2007 water year (spring/early summer and late summer/fall) were averaged for the bulk of our analyses; however, to test the sensitivity of results to sampling time, a set of source-mixing analyses were also conducted using the individual sample values. For the remaining lakes, the data represent a single sampling event during the spring, summer, or fall of 2007. To facilitate identification of contributing catchment areas and calculation of model parameters within those areas, a 2-step process was used to reposition sampling site coordinates onto a 1-km stream network grid that was derived from the USGS Hydro-1K terrain model (data available from the U.S. Geological Survey: <https://lta.cr.usgs.gov/HYDRO1K>) using TauDEM 5.3.7 (<http://hydrology.usu.edu/taudem/taudem5/>). First, sampling sites were associated with their lake-area polygon representation from the NHDPlusV2 geodatabase (<https://www.epa.gov/waterdata/nhdplus-national-data>), and if the gridded stream network included a stream (here defined as a point draining an area of 25 km<sup>2</sup> or larger) within that polygon the sampling point was relocated to the highest-flow (i.e., outlet) grid cell within the lake polygon. For many smaller lakes the gridded stream network did not route a stream through the NHD lake polygon, and these sites were snapped to the closest stream down-slope from their original location using

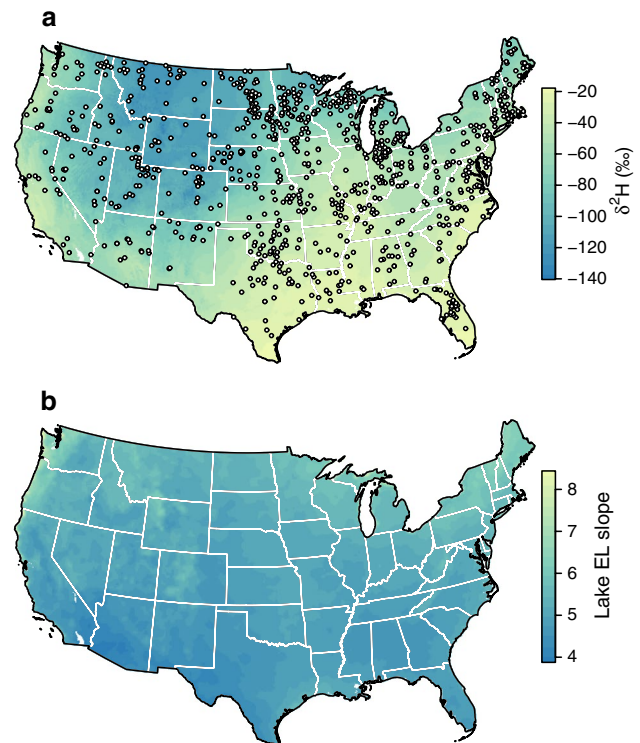


**Fig. 7** New data products developed for the lake iSW<sub>E</sub> application. **a** Example high-resolution (1 km) precipitation isoscape for the month of October (climatological). Points show the location of 925 lakes included in the analyses. **b** Modeled surface water evaporation line slopes for the 2007 water year. Estimates represent the evaporation amount-weighted average of slopes calculated for each month, as described in the text. This figure is available in color in the online version of the journal

the “moveoutletstostreams” tool in TauDEM. Eliminating 16 sites that could not be reconciled with the stream network, the final dataset consisted of values for 1141 lakes, 925 of which we considered to exhibit significant evapoconcentration effects (lake water *D*-excess value more than 5‰ below the estimated precipitation source water value).

To estimate isotope ratios of precipitation inputs, we produced new precipitation isoscapes (spatial models) at 1-km resolution for the contiguous USA and adjacent areas (Fig. 7a). These were generated using the method and algorithms of Bowen (2008) and Bowen and Revenaugh (2003), and a dataset of monthly precipitation isotope data from the region bounded by 18° < latitude < 51° and −145° < longitude < −57°. In brief, isotopic data from individual precipitation monitoring sites were used to fit a hybrid regression/interpolation model, parameterized in terms of effective latitude (latitude adjusted for seasonal migration of the inter-tropical convergence zone) and its square, elevation, and an interpolation distance-weighting parameter. The model was then applied across the study area to make predictions. Isotopic data were compiled from sources including the U.S.

Network for Isotopes in Precipitation (Welker 2000), Global Network for Isotopes in Precipitation (IAEA/WMO 2011), and published and unpublished work, giving between 104 and 119 sites for individual months and 190 and 192 sites for annual average  $\delta^2\text{H}$  and  $\delta^{18}\text{O}$ , respectively. Locations and information on the monitoring sites, along with access to all data for which we have been granted redistribution permission, is available through the Waterisotopes Database portal ([http://wateriso.utah.edu/waterisotopes/pages/spatial\\_db/SPATIAL\\_DB.html](http://wateriso.utah.edu/waterisotopes/pages/spatial_db/SPATIAL_DB.html)). The gridded isoscapes were created using the Hydro1K elevation grid and are available at [http://wateriso.utah.edu/waterisotopes/pages/data\\_access/ArcGrids.html](http://wateriso.utah.edu/waterisotopes/pages/data_access/ArcGrids.html).

Precipitation isotope values were averaged within the runoff contributing areas for each lake using the flow accumulation tool in TauDEM. Annual, winter (October–March), and summer (April–September) averages were calculated, weighting the monthly value at each gridcell by precipitation–evaporation ( $P-E$ , here referred to as “runoff”) from the North American Regional Reanalysis (NARR, Mesinger et al. 2006; <http://www.esrl.noaa.gov/psd/>). This procedure implicitly assumes that evaporation from each grid cell is derived from the current month’s precipitation, ignoring potential carry-over between months that may bias runoff ratios over the seasonal cycle and be detectable using  $i\text{SW}_E$ . To avoid numerical errors associated with small values raw NARR monthly  $P$  and  $E$  values less than zero were set to zero and  $P-E$  was set to the larger of the NARR value or  $0.001 \text{ kg/m}^2/\text{month}$ .

We also generated new gridded estimates of evaporation-weighted EL slopes across the study region (Fig. 7b). We used gridded climate data from the NARR to calculate equilibrium (Horita and Wesolowski 1994) and kinetic fractionation factors (Gat 1996) for evaporation during each calendar month of the 2007 water year. Atmospheric water vapor isotope ratios were estimated using the monthly precipitation isotope ratios and equilibrium fractionation factors for each grid cell (Gibson et al. 2008). Evaporation slopes were then calculated using Eq. 7 of Gat and Bowser (1991; also see Eq. 7 of Gat 1996) and averaged, with monthly weighting by the NARR surface evaporation flux to reflect seasonal differences in evaporation rates (e.g., Gibson et al. 2008). Grids were created for both soil and surface water evaporation, with the kinetic fractionation effect for surface waters being 50% of that for soils due to greater turbulent transport within the boundary layer above open water bodies (Craig and Gordon 1965; Gat 1996). General patterns and mean values of EL slopes mapped here are consistent with previous estimates, although the range of values predicted and their sensitivity to climate parameters is somewhat larger (Gibson et al. 2008). The gridded estimates of EL slopes, including the 2007 surface water evaporation grids used here, a soil water EL grid, and a set of climatological average

grids generated using the same method, are available for download at [http://wateriso.utah.edu/waterisotopes/pages/data\\_access/ArcGrids.html](http://wateriso.utah.edu/waterisotopes/pages/data_access/ArcGrids.html).

We conducted single-source and mixture analyses on the lake water data using the  $i\text{SW}_E$  routines described above. For the single-source analysis, we used catchment-averaged, runoff-weighted mean annual precipitation isotope ratios to represent the hypothesized source waters, with H and O standard deviations and covariance value estimated to be approximately {4, 0.5, 0.8} based on the average uncertainty of the precipitation isoscapes. Observed lake water isotope ratios were used for the sample values, with an uncertainty of {2.7, 0.58, 0.95} estimated from the average variance and covariance of repeat samples from 95 of the lakes within the dataset. We assumed that the majority of the evapoco-concentration experienced by the samples happened within the local lake environment, and used the estimated lake water EL slope value at the site of sampling as the mean value for  $m_t$ . Uncertainty in  $m_t$  arises from a range of factors, including representativeness of the climate data used, uncertainty in the atmospheric water vapor isotope ratios, and potential influence of soil–water evaporation. Lacking a systematic estimate of uncertainty, we use a  $1\sigma$  value of 0.5, equal to the standard deviation of mean  $m_t$  values estimated across all sampling sites. Parameter values in the mixtures analysis were identical, with the exception of the hypothesized sources; in this case the catchment-averaged, runoff-weighted summer and winter precipitation values were used for the two endmember source values and the prior estimate of the fractional contribution of each was calculated as the ratio of the catchment runoff for the two seasons. 10,000 Monte Carlo draws were conducted for each sample for the single-source example, and 10,000 posterior draws were obtained for the mixing analyses.

## Results

Isotopic data for the majority of the surveyed lakes were broadly consistent with source water isotope ratios equal to the runoff-weighted annual average precipitation from the lake’s catchment. The relative conditional probability value, representing the  $i\text{SW}_E$  support for the hypothesized source, averaged 0.38 across the entire dataset. However, for 94 of the 925 lakes (10%) the average relative conditional probability was less than 0.05, providing strong evidence for a source water composition different than that of catchment-averaged runoff. This total was somewhat higher (263, 28%) when the median of the conditional probability distribution was considered, reflecting a subset of samples for which a substantial number of draws from the prior distributions

produced source water values higher than the sample values (and thus a conditional probability of zero).

The strength of evidence for/against the hypothesized annual average water source was not randomly distributed: in general, lakes that had lower  $\delta^{18}\text{O}_o$  values tended to give lower relative conditional probabilities (Fig. 8a; *F* test,  $p \ll 0.001$ ). Conditional probability was also correlated with lake water *D*-excess value (Fig. 8b;  $p \ll 0.001$ ), but this relationship explained a fairly small fraction of variance (9 vs 26% for  $\delta^{18}\text{O}_o$ ) suggesting that the observed correlation with  $\delta^{18}\text{O}_o$  was not solely an artifact of differences in evapoconcentration between low- and high- $\delta^{18}\text{O}$  lakes. As expected given the correlation with lake water  $\delta^{18}\text{O}$ , low-probability results were geographically clustered (Fig. 9a). Very few lakes in the southern and southeastern USA gave strong evidence for a water source other than annual average runoff. Clusters of low-probability sites existed throughout the Western Interior, Pacific Northwest, central Great Plains, Great Lakes region, lower Ohio River Valley, and New England. Mean conditional probability was very weakly correlated with estimated EL slope (adjusted  $r^2 < 0.02$ ).

Mixing analyses were obtained for 69 lakes with replicate early and late-season sampling; for the other 26 repeat-sampled lakes one or more sample was not significantly evaporated or failed to converge on a well-constrained mixing ratio. Mean estimated winter water fractions obtained from the early and late-season samples were strongly correlated (adjusted  $r^2 = 0.97$ ; *F* test,  $p \ll 0.001$ ), with no significant difference between estimates for the two sampling bouts (mean difference = 0.9%; *T* test,  $p = 0.06$ ). Mixing analysis for the entire dataset suggested a slightly larger fraction of winter water in lakes than estimated based on the NARR annual runoff estimates (mean posterior across all sites was

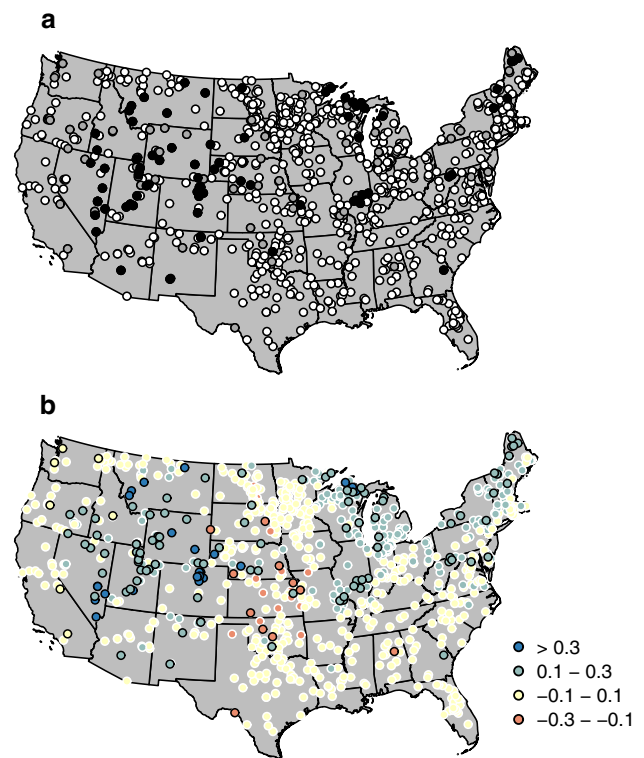


**Fig. 9** Spatial distribution of  $i\text{SW}_E$  results for lake samples. **a** Sites with mean single-source conditional probabilities less than 0.1 (gray fill) or 0.05 (black), providing support for source water compositions different from that of runoff-weighted annual precipitation. All other sites plotted with white fill. **b** Winter bias of lake water inflow, based on mixture analysis. Plotted values are the estimated fraction of winter water (mean of the posterior mixtures distribution) minus the NARR-estimated fraction of winter runoff within the lake’s catchment (i.e., mean of the prior). Black symbol outlines show sites for which the mean conditional probability in the single-source analysis was less than 0.1. This figure is available in color in the online version of the journal

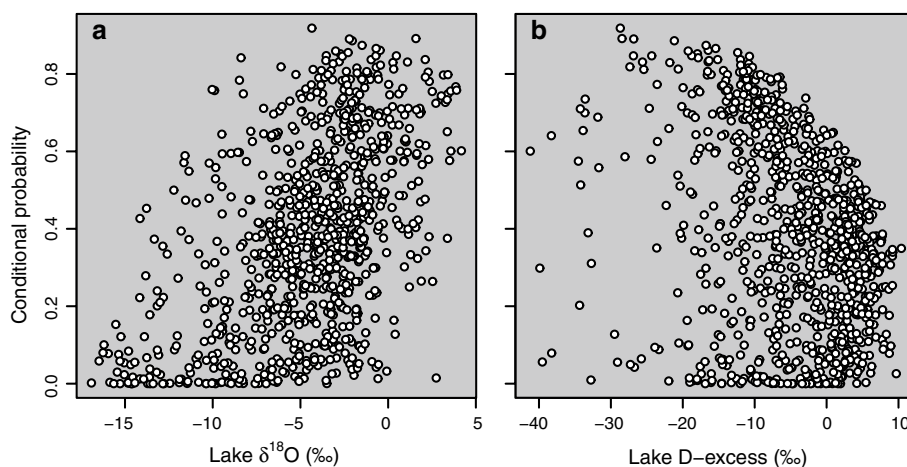


**Fig. 8** Mean conditional probability values from single-source  $i\text{SW}_E$  analysis of lake water isotope data. **a** Conditional probabilities of the hypothesized source water values are correlated with lake water isotope ratios, with lakes in lower- $\delta^{18}\text{O}$  settings (e.g., cooler, higher)

less likely to hold water that is isotopically similar to annual runoff-weighted average precipitation within their catchments. **b** The correlation shown in a is independent of the lake water deuterium excess, and thus the amount of evapoconcentration of the lake water

0.54, vs. a mean value of 0.47 for the prior). Posterior means were higher than prior means for the winter contribution to lake water for 640 of the 906 sites where the analysis converged (71%) and for 124 of 136 sites with single-source mean conditional probabilities less than 0.1 (91%). The isotopic analysis suggested that the NARR annual runoff estimate (the prior) underestimated the fraction of winter water at most sites where winter runoff provided more than half of the lake inflow, whereas there was a tendency for the prior to overestimate winter contributions for some lakes where less than 40% of inflow was winter-sourced (Fig. 10). The degree of under- or overestimation for winter-dominated lakes was larger than that for summer-dominated ones.

The distribution of winter lake water bias (calculated as described in the previous paragraph) showed strong spatial structure (Fig. 9b). Underestimation of the winter contribution to lake water using the runoff prior is prevalent throughout the western interior, Midwest, and New England. The majority of lakes for which winter inflow is overestimated lie in the central Great Plains. Most lakes in the Pacific Coast, South, and northern Great Plains exhibit limited winter bias.

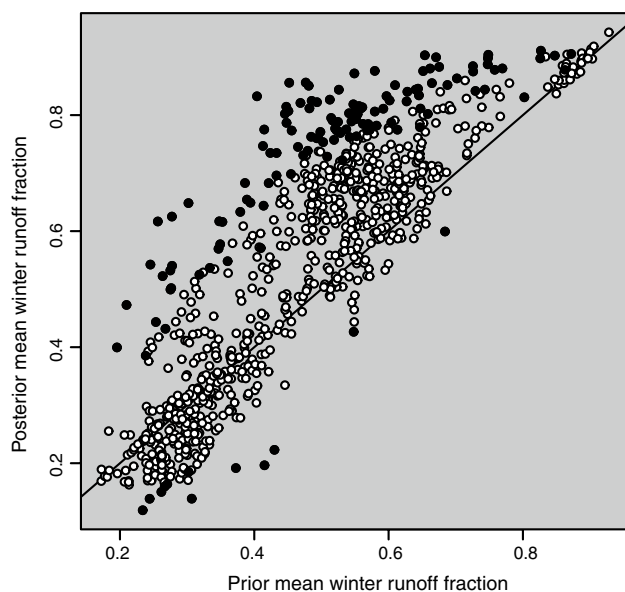


**Fig. 10** Results of the mixtures analysis of lake waters, showing the mean value of the prior for the winter source (equal to the fraction of annual NARR-estimated runoff occurring during winter months) and the posterior distribution estimated from the  $iSW_E$  mixing analysis. Black-filled symbols show sites for which the mean conditional probability in the single-source analysis was less than 0.1. The 1:1 line is shown

## Discussion

### $iSW_E$ application

We successfully applied two of the three  $iSW_E$  algorithms to a large lake water isotope dataset to draw inferences about water sources to lakes. Gridded data products provided model inputs and produced valid and reasonable (see below) results for most sites. A small number of sites were discarded because they could not be reconciled with the terrain model-derived stream network, and for 17 samples the mixing model analysis was aborted because too few valid draws were obtained. This result generally reflected a poorly posed mixing scenario, where the hypothesized sources (NARR summer and winter predicted runoff) did not bracket the most likely true source water values (predicted EL intercept of the MWL). Processing time was longest for the mixing analysis but tractable, taking less than 4 h to complete all 925 samples running in parallel on 8 cores of an Intel i7-3820 processor. Analysis time could be improved by adopting a more efficient Markov Chain Monte Carlo sampler, and further exploration of convergence and stability of the models could support additional optimization of sampling.

Our results demonstrate one outcome that signals a potential mode of misuse. Output from the single-source analysis shows a decreasing upper bound on the conditional probability as lake water  $d$  values increase toward 10‰ (Fig. 8b). This reflects the fact that as the isotopic separation between the lake water and the GMWL, and thus the hypothesized source, decreases, a fraction of the draws from the prior distributions produce source values with one or both isotope ratios higher than those of the lake sample, giving a conditional probability of zero (Eq. 1b). Although the contribution of these draws limits the maximum mean conditional probabilities obtained, in general a clear distinction can still be drawn between samples for which the hypothesized source is a good fit to the  $iSW_E$  model and those where it is not (Fig. 8b). In actuality, the algorithm is giving conditional probabilities for these samples that accurately reflect the goal of the analysis: providing information on the likelihood that the lake sample was derived from the hypothesized source with evaporation. In these cases, however, there is overlap between the source and sample distributions, reflecting the possibility that the sample was derived from the source without evaporation. Additional analysis components could be added to incorporate this information, but users of the tools and approach proposed here should be aware of and critically evaluate the appropriateness of this nuance of the analysis framework.

## Lake water sources

The results of our analyses suggest that the isotopic composition of lake water in a substantial fraction of US lakes is not an unbiased integration of catchment  $P-E$  weighted monthly precipitation. Moreover, we suggest that pervasive and non-random bias in seasonal inputs to lakes exists across parts of the USA, with a tendency for winter precipitation to be over-represented in cold and snow-prone regions and summer precipitation over-represented across part of the Great Plains. This result is in contrast with previous work suggesting limited bias or summer-bias for lakes within the western USA (Henderson and Shuman 2009, 2010), and more consistent with results from rivers (Henderson and Shuman 2010). Both lake analyses used samples collected primarily in the summer and fall seasons, and although they may not be totally representative of full-year water balance of the lakes they should be broadly comparable. In addition, our paired mixing analyses of samples from early and late-season collections at 69 lakes show no detectable seasonal bias. Our analysis differs from the previous work in terms of the nature and scope of the dataset, the use of theoretically predicted ELs as opposed to ELs fit to water samples from multiple lakes, the resolution and currency of the gridded data products used, and the analytical and uncertainty analysis framework used, any or all of which may have contributed to the difference in results. Although comprehensive sensitivity testing of our result is beyond this scope of this paper we have shown that our results are not strongly affected by variation in our modeled EL slopes, one potential source of bias. We also note that the EL slope estimation process used in Henderson and Schuman is susceptible to bias associated with source water isotope variation, as discussed here and illustrated in Fig. 1c. A common winter-bias for lakes and rivers would be less enigmatic than the previously proposed dichotomy given that lakes and streams are fundamentally flow-connected, but further work on both types of systems using comparable methods and more exhaustive interrogation of results should be conducted before firm conclusions are drawn.

The suggestion of seasonal source water bias implies a carry-over contribution of precipitation from the over-represented season to runoff entering the lakes during the under-represented season, and conversely a carry-over contribution from the under-represented season to evapotranspiration (ET) during the over-represented season. For the dominant winter-biased lake basins, this would be consistent with summer-derived precipitation contributing more strongly to the ET flux during fall months than snowmelt does to spring and early summer ET. Winter recharge has been argued to contribute disproportionately to many groundwater reservoirs (Bowen et al. 2012; Jasechko et al. 2014), and efficient infiltration and groundwater recharge by melting snowpack

provides a plausible mechanism for the observed effect that is also qualitatively consistent with the spatial distribution of winter-biased lakes (Fig. 9b). Summer-biased lakes, less common in our analysis, occurred in regions where snowpack is less persistent and strong summer storms are important contributors to precipitation, and could be explained through a similar mechanism by which summer storm water is more likely to contribute to recharge and winter-derived moisture sustains a substantial fraction of spring and summer ET. Both patterns of seasonal bias suggest that changes in climate could change how lake water integrates isotopic information from within its catchment. Although most lakes appear to be robust and consistent integrators, the potential for such changes could impart systematic bias to paleoclimatic and paleoecological archives from lake sediments and should be factored into interpretation of such records.

## Conclusion

Inference of water source is a powerful and pervasive application of water isotopes, and analysis frameworks that accommodate evapoconcentration effects are necessary for many systems. Critical assessment of the assumptions inherent in any such analysis framework is needed, and applications that potentially violate assumptions associated with the estimation of evaporation line slopes are not uncommon in the literature and may in some cases have produced biased results. We recommend use of theoretical approaches to estimate EL slopes (Craig–Gordon model) unless data are available that unambiguously reflect evapoconcentration effects without the complicating influence of source water isotope variation. In some situations, use of a regression approach cross-checked by theoretical calculations might prove useful for demonstrating of the validity of the regression EL slope, given these concerns. Uncertainty estimation is another challenge in these studies, and most previous work has not provided rigorous quantification of uncertainty. We propose a new, simplified framework for these  $iSW_E$  analyses that is conducive to robust and comprehensive uncertainty estimation and promotes explicit specification and testing of source water hypotheses. The framework is implemented as a set of tools in the R programming language that are suitable for use in many study systems. Application of the tools to a large dataset for US lakes suggests that many lakes are not unbiased integrators of precipitation within their catchments, and in particular lakes in snow-prone regions appear to contain a larger fraction of winter precipitation than would be inferred from winter and summer season precipitation–evaporation balance. This implies an asymmetric significance of seasonal precipitation in the water budget of lake basins, with implications for sensitivity of aquatic

ecosystems, paleolimnological proxies, and water resource to winter and summer precipitation change. Future application of the framework proposed here could reveal equivalent sensitivities elsewhere within ecohydrological systems and provide generalized and system-specific information about plant, soil, surface and groundwater response to seasonal precipitation inputs.

**Acknowledgements** The authors are tremendously grateful for the inspiration, support, and mentorship of Jim Ehleringer, whose creativity and enthusiasm for science has impacted each of us and so many other young scientists worldwide. Support for this work was provided by U.S. National Science Foundation Grants EF-01241286 and DBI-1565128 to GJB. This manuscript has been subjected to Agency review and has been approved for publication. The views expressed in this paper are those of the author(s) and do not necessarily reflect the views or policies of the U.S. Environmental Protection Agency. Mention of trade names or commercial products does not constitute endorsement or recommendation for use.

**Author contribution statement** GJB, DRB, EJO, and SPG conceived the study. GJB designed and performed the analyses. AP managed and prepared data. JRB provided data. GJB and JRB wrote the manuscript; other authors provided editorial advice.

**Funding** Funding was provided by the U.S. National Science Foundation Directorate for Biological Sciences (EF-01241286 and DBI-1565128).

## Compliance with ethical standards

**Conflict of interest** The authors declare no conflict of interest.

## References

- Bijoor NS, McCarthy HR, Zhang D, Pataki DE (2012) Water sources of urban trees in the Los Angeles metropolitan area. *Urban Ecosyst* 15:195–214. <https://doi.org/10.1007/s11252-011-0196-1>
- Bowen GJ (2008) Spatial analysis of the intra-annual variation of precipitation isotope ratios and its climatological corollaries. *J Geophys Res* 113:D05113. <https://doi.org/10.1029/2007JD009295>
- Bowen GJ, Good SP (2015) Incorporating water isoscapes in hydrological and water resource investigations. *Wiley Interdiscip Rev Water* 2:107–119
- Bowen GJ, Revenaugh J (2003) Interpolating the isotopic composition of modern meteoric precipitation. *Water Resour Res* 39:1299. <https://doi.org/10.1029/2003WR002086>
- Bowen GJ, Wilkinson B (2002) Spatial distribution of  $\delta^{18}\text{O}$  in meteoric precipitation. *Geology* 30:315–318
- Bowen GJ, Kennedy CD, Henne PD, Zhang T (2012) Footprint of recycled water subsidies downwind of Lake Michigan. *Ecosphere* 3(6):53. <https://doi.org/10.1890/ES12-00062.1>
- Brooks JR, Barnard HR, Coulombe R, McDonnell JJ (2010) Ecohydrologic separation of water between trees and streams in a Mediterranean climate. *Nat Geosci* 3:100–104. <https://doi.org/10.1038/NNGEO722>
- Brooks JR, Gibson JJ, Birks SJ, Weber MH, Rodecap KD, Stoddard JL (2014) Stable isotope estimates of evaporation: inflow and water residence time for lakes across the United States as a tool for national lake water quality assessments. *Limnol Oceanogr* 59:2150–2165
- Chesson LA, Bowen GJ, Ehleringer R (2010) Analysis of the hydrogen and oxygen stable isotope ratios of beverage waters without prior water extraction using isotope ratio infrared spectroscopy. *Rapid Commun Mass Spectrom* 24:3205–3213. <https://doi.org/10.1002/rcm.4759>
- Clark I, Fritz P (1997) *Environmental isotopes in hydrogeology*. Lewis, Boca Raton
- Corbin JD, Thomsen MA, Dawson TE, D'Antonio CM (2005) Summer water use by California coastal prairie grasses: fog, drought, and community composition. *Oecologia* 145:511–521. <https://doi.org/10.1007/s00442-005-0152-y>
- Craig H (1961) Isotopic variations in meteoric waters. *Science* 133:1702–1703
- Craig H, Gordon LI (1965) Deuterium and oxygen-18 variations in the ocean and the marine atmosphere. In: Tongiorgi E (ed) *Proceedings of a conference on stable isotopes in oceanographic studies and paleotemperatures*, Spoleto, Italy, vols 9–130
- Dansgaard W (1964) Stable isotopes in precipitation. *Tellus* 16:436–468
- Dawson TE (1998) Fog in the California redwood forest: ecosystem inputs and use by plants. *Oecologia* 117:476–485
- Dawson TE, Ehleringer JR (1991) Streamside trees that do not use stream water. *Nature* 350:335–337
- Dawson TE, Pate JS (1996) Seasonal water uptake and movement in root systems of Australian phreatophytic plants of dimorphic root morphology: a stable isotope investigation. *Oecologia* 107:13–20. <https://doi.org/10.1007/bf00582230>
- Ehleringer JR, Dawson TE (1992) Water uptake by plants: perspectives from stable isotope composition. *Plant Cell Environ* 15:1073–1082
- Ehleringer JR, Phillips SL, Schuster WSF, Sandquist DR (1991) Differential utilization of summer rains by desert plants. *Oecologia* 88:430–434. <https://doi.org/10.1007/bf00317589>
- Ehleringer JR, Barnette JE, Jameel Y, Tipple BJ, Bowen GJ (2016) Urban water—a new frontier in isotope hydrology. *Isot Environ Health Stud* 52:477–486. <https://doi.org/10.1080/10256016.2016.1171217>
- Ellsworth PZ, Williams DG (2007) Hydrogen isotope fractionation during water uptake by woody xerophytes. *Plant Soil* 291:93–107. <https://doi.org/10.1007/s11104-006-9177-1>
- Evaristo J, Jasechko S, McDonnell JJ (2015) Global separation of plant transpiration from groundwater and streamflow. *Nature* 525:91–94
- Gat JR (1996) Oxygen and hydrogen isotopes in the hydrologic cycle. *Annu Rev Earth Planet Sci* 24:225–262
- Gat JR, Bowser CJ (1991) The heavy isotope enrichment of water in coupled evaporative systems. In: Taylor HP, O'Neil JR, Kaplan IR (eds) *Stable isotope geochemistry: a tribute to samuel Epstein*. The Geochemical Society, St. Louis, pp 159–168
- Gibson JJ, Birks SJ, Edwards TWD (2008) Global prediction of  $\delta_A$  and  $\delta^2\text{H}-\delta^{18}\text{O}$  evaporation slopes for lakes and soil water accounting for seasonality. *Glob Biogeochem Cycles* 22:GB2031. <https://doi.org/10.1029/2007gb002997>
- Goldsmith GR, Muñoz-Villers LE, Holwerda F, McDonnell JJ, Asbjornsen H, Dawson TE (2012) Stable isotopes reveal linkages among ecohydrological processes in a seasonally dry tropical montane cloud forest. *Ecohydrology* 5:779–790
- Good SP et al (2014) Patterns of local and non-local water resource use across the western United States determined via stable isotope intercomparisons. *Water Resour Res*. <https://doi.org/10.1002/2014WR015884>
- Good SP, Noone D, Bowen GJ (2015a) Hydrologic connectivity constrains partitioning of global terrestrial water fluxes. *Science* 349:175–177. <https://doi.org/10.1126/science.aaa5931>

- Good SP, Noone D, Kurita N, Benetti M, Bowen GJ (2015b) D/H isotope ratios in the global hydrologic cycle. *Geophys Res Lett.* <https://doi.org/10.1002/2015GL064117>
- Henderson AK, Shuman BN (2009) Hydrogen and oxygen isotopic compositions of lake water in the western United States. *Geol Soc Am Bull* 121:1179–1189. <https://doi.org/10.1130/B26441>
- Henderson AK, Shuman BN (2010) Differing controls on river- and lake-water hydrogen and oxygen isotopic values in the western United States. *Hydrol Process* 24:3894–3906
- Horita J, Wesolowski DJ (1994) Liquid-vapor fractionation of oxygen and hydrogen isotopes of water from the freezing to the critical temperature. *Geochim Cosmochim Acta* 58:3425–3437
- IAEA/WMO (2011) Global network of isotopes in precipitation. The GNIP Database. <http://www.iaea.org/water>. Accessed 11 Oct 2011
- Jameel Y, Brewer S, Good SP, Tipple BJ, Ehleringer JR, Bowen GJ (2016) Tap water isotope ratios reflect urban water system structure and dynamics across a semiarid metropolitan area. *Water Resour Res.* <https://doi.org/10.1002/2016WR019104>
- Jasechko S et al (2014) The pronounced seasonality of global groundwater recharge. *Water Resour Res* 50:8845–8867. <https://doi.org/10.1002/2014WR015809>
- Kendall C, Coplen TB (2001) Distribution of oxygen-18 and deuterium in river waters across the United States. *Hydrol Process* 15:1363–1393
- Kendall C, McDonnell JJ (eds) (1998) *Isotope tracers in catchment hydrology*. Elsevier, Amsterdam
- Lin G, Sternberg L, Ehleringer J, Hall A, Farquhar G (1993) Hydrogen isotopic fractionation by plant roots during water uptake in coastal wetland plants. In: Ehleringer JR, Hall AE, Farquhar GD (eds) *Stable isotopes and plant carbon–water relations*. Academic Press, New York, pp 497–510
- Mesinger F et al (2006) North american regional reanalysis. *Bull Am Meteorol Soc* 87:343–360. <https://doi.org/10.1175/BAMS-87-3-343>
- Oerter EJ, Bowen G (2017) In situ monitoring of H and O stable isotopes in soil water reveals ecohydrologic dynamics in managed soil systems. *Ecohydrology* 10:e1841
- Oerter E, Finstad K, Schaefer J, Goldsmith GR, Dawson T, Amundson R (2014) Oxygen isotope fractionation effects in soil water via interaction with cations (Mg, Ca, K, Na) adsorbed to phyllosilicate clay minerals. *J Hydrol* 515:1–9
- Oerter E, Malone M, Putman A, Drits-Esser D, Stark L, Bowen G (2017) Every apple has a voice: using stable isotopes to teach about food sourcing and the water cycle. *Hydrol Earth Syst Sci* 21:3799–3810. <https://doi.org/10.5194/hess-21-3799-2017>
- Roden JS, Ehleringer JR (2007) Summer precipitation influences the stable oxygen and carbon isotopic composition of tree-ring cellulose in *Pinus ponderosa*. *Tree Physiol* 27:491–501
- Rozanski K, Araguas-Araguas L, Gonfiantini R (1993) Isotopic patterns in modern global precipitation. In: Swart PK, Lohmann KC, McKenzie J, Savin S (eds) *Climate change in continental isotopic records*. American Geophysical Union, Washington, DC, pp 1–36
- R Core Team (2017) R: a language and environment for statistical computing. R Foundation for Statistical Computing, Vienna. <https://www.R-project.org/>. Accessed 7 Jan 2017
- Tipple BJ et al (2017) Stable hydrogen and oxygen isotopes of tap water reveal structure of the San Francisco Bay Area's water system and adjustments during a major drought. *Water Res* 119:212–224. <https://doi.org/10.1016/j.watres.2017.04.022>
- Welhan JA, Fritz P (1977) Evaporation pan isotopic behavior as an index of isotopic evaporation conditions. *Geochim Cosmochim Acta* 41:682–686. [https://doi.org/10.1016/0016-7037\(77\)90306-4](https://doi.org/10.1016/0016-7037(77)90306-4)
- Welker JM (2000) Isotopic ( $\delta^{18}\text{O}$ ) characteristics of weekly precipitation collected across the USA: an initial analysis with application to water source studies. *Hydrol Process* 14:1449–1464
- Williams DG, Coltrain JB, Lott MJ, English NB, Ehleringer JR (2005) Oxygen isotopes in cellulose identify source water for archaeological maize in the American Southwest. *J Archaeol Sci* 32:931–939. <https://doi.org/10.1016/j.jas.2005.01.008>
- Zhao L et al (2016) Significant difference in hydrogen isotope composition between xylem and tissue water in *Populus euphratica*. *Plant Cell Environ* 39:1848–1857